

Localization of Dirac electrons by Moiré patterns in graphene bilayers

Guy Trambly de Laissardière,^{1,*} Didier Mayou,² and Laurence Magaud²

¹*Laboratoire de Physique Théorique et Modélisation,*

Université de Cergy-Pontoise – CNRS, F-95302 Cergy-Pontoise Cedex, France.

²*Institut Néel, CNRS – Université Joseph Fourier, F-38042 Grenoble, France*

(Dated: May 29, 2018)

We study the electronic structure of two Dirac electron gazes coupled by a periodic Hamiltonian such as it appears in rotated graphene bilayers. *Ab initio* and tight-binding approaches are combined and show that the spatially periodic coupling between the two Dirac electron gazes can renormalize strongly their velocity. We investigate in particular small angles of rotation and show that the velocity tends to zero in this limit. The localization is confirmed by an analysis of the eigenstates which are localized essentially in the AA zones of the Moiré patterns.

PACS numbers: 73.20.-r, 73.20.At, 73.21.Ac, 81.05.Uw

Introduction.– Graphene is a two dimensional carbon material which takes the form of a planar lattice of sp^2 bonded atoms. Its honeycomb lattice consists in two sublattices which gives a specific property to the wave function, the so-called chirality. The linear dispersion relation close to the charge neutrality point implies that, in this energy range, the electrons obey an effective massless Dirac equation [1, 2, 3]. The properties of electrons in graphene, deriving from the Dirac equation, are fundamentally different from those deriving from the Schrödinger equation. In particular the quantum Hall effect is quantized with integer plus half values [4, 5] and can even be observed at room temperature [6]. Another example of the unique behavior of Dirac electrons is the so-called Klein paradox which is intimately related to the chirality of their wavefunction. The Klein paradox is the fact that, in a one-dimensional configuration, a potential barrier is perfectly transparent for electrons. As a consequence it is difficult to localize Dirac electrons with an electrostatic potential, although it can be of great interest to realize this confinement, in particular for the production of elementary devices [7, 8].

Therefore it is necessary to improve our knowledge of the behavior of Dirac electrons in various types of potentials. For disordered potentials specific behavior related to the chirality of Dirac electrons, such as weak anti-localization effects, have been predicted theoretically [9] and observed in epitaxial graphene [10, 11, 12, 13]. Recent STM measurements, performed on epitaxial graphene, have also confirmed the absence of backscattering related to the Klein paradox [14]. For periodic systems several studies have been published concerning either a simple graphene sheet in an applied periodic potential or periodic bilayers [15, 16]. The bilayer system [17, 18, 19, 20] has shown an unexpected and rich behaviour. The well-known Bernal AB stacking leads to massive quasiparticles with quadratic dispersion close to the Dirac point. Yet it has been recognized recently in the scientific community that another important case is that of rotated graphene bilayers, which are observed for

example in epitaxial graphene on the C-terminated face of SiC [17]. In a rotated bilayer the superposition of the two rotated honeycomb lattices generates a Moiré pattern with a longer period. The two Dirac electron gazes are then coupled by a periodic interaction, with a large supercell, which can restore a Dirac-like linear dispersion. However fundamental issues are controversial. In particular Lopez dos Santos *et al.* [18] have shown, with a perturbative treatment of the interplane coupling, that the velocity can be renormalized and tend to decrease in a rotated bilayer with respect to its value in pure graphene. In contrary Shallcross *et al.* [19] conclude from *ab initio* calculations and from some general arguments that the velocity is unchanged in rotated graphene bilayers.

In this letter we combine *ab initio* and tight-binding (TB) approaches and conclude indeed that there is a renormalization of the velocity for bilayers as compared to pure graphene. Most importantly the velocity tends to zero in the limit of small twist angles which means that this type of coupling is able to confine the two Dirac electron gazes. We also show that the electronic wavefunction tends to localize in regions of the bilayer which are locally similar to the AA arrangement. This new localization regime should be observable since angles as small as a fraction of a degree, for which we predict strong localization effects, are found in some rotated multilayers. In particular large Moiré patterns have been observed on STM image of graphene multilayers on top of SiC C-face [21] and also on graphite [22]. Our work demonstrates also that the perturbative theory of Lopez dos Santos *et al.* [18] is correct for angles greater than typically 3 degrees but cannot deal with the remarkable localization phenomenon that occurs in the limit of small twist angles.

Moiré patterns and geometry of rotated bilayer.– Moiré Patterns can be obtained in two cases: when two lattices with slightly different parameters are superimposed or when two identical lattices are rotated by an angle θ [23]. The present situation corresponds to the later case. A commensurate structure can be defined if the rotation

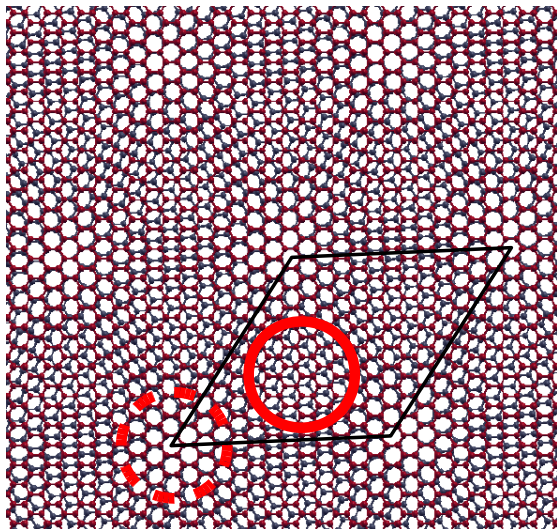


FIG. 1: (color on line) Commensurate bilayer cell $(n, m) = (6, 7)$ for a rotation of $\theta = 5.08^\circ$. Full (dashed) line circle AB (AA) region.

changes a lattice vector $\mathbf{V}(m, n)$ to $\mathbf{V}'(n, m)$ with n, m the coordinates with respect to the basis vectors \vec{a}_1 ($\sqrt{3}/2, -1/2$) and \vec{a}_2 ($\sqrt{3}/2, 1/2$). The rotation angle is then defined as follows:

$$\cos \theta = \frac{n^2 + 4nm + m^2}{2(n^2 + nm + m^2)} \quad (1)$$

and the commensurate cell vectors correspond to :

$$\vec{t} = \mathbf{V}' = n\vec{a}_1 + m\vec{a}_2 \quad ; \quad \vec{t}' = -m\vec{a}_1 + (n+m)\vec{a}_2. \quad (2)$$

The commensurate unit cell contains $N = 4(n^2 + nm + m^2)$ atoms. It is important to notice that $\theta \sim 0$ results in a large cell –large n and m – and small $|m - n|$. Large commensurate cells can be also obtained for large angles $\theta \sim 30^\circ$ then $|m - n|$ is large [23]. $\theta = 60^\circ$ is the perfect AB stacking and θ close to 60° is obtained for $n = 1$ ($m = 1$) and large m (n).

For small angle, if the rotation axis, perpendicular to the planes, passes through atomic positions in both layers (figure 1), atoms in the 4 corners of the supercell are directly superimposed (figure 1). This corresponds to the so-called AA stacking. For $(n, m = n + 1)$ cells, zone with AB stacking –graphite like stacking– are located at $1/3$ and $2/3$ of the long diagonal (figure 1).

Quite generally the structures that we study are fully characterized by the two index (n, m) of the rotation and also by the value of the translation vector between the two layers. However for sufficiently small values of the rotation angle θ the Moiré pattern depends essentially on the rotation angle and the translation of one layer only results in a rigid shift of the overall Moiré structure. Also in the small angle limit, all dimensions of the Moiré pattern scale like $1/\theta$ and in particular the size of locally AA

or AB stacked regions and the distance between these zones are proportional to $1/\theta$.

Let us emphasize that the limit of small angle is discontinuous: when the rotation angle decreases the dimensions of the Moiré structure scale like $1/\theta$ and therefore the structure does not tend to that for exactly zero angle. This singular, discontinuous, geometric evolution is associated to singular electronic properties as we show in this work.

Ab-initio and tight-binding methods for electronic structure.– Our approach combines *ab initio* calculations that can be used for unit cells containing up to 500-600 atoms and tight-binding (TB) calculations that can be used for unit cells containing up to 15000 atoms or even more. *Ab initio* calculations are performed with the code VASP [24] and the generalized gradient approximation [25]. The C ultra soft pseudopotential [26] has been extensively tested previously [17, 21]. The plane wave basis cutoff is equal to 211 eV. The empty space width is equal to 21 Å, the interlayer distance is fixed to its experimental value ($\simeq 3.35$ Å) and no atom are allowed to relax for direct comparison with TB calculations.

In the tight-binding scheme only p_z orbitals are taken into account since we are interested in electronic states close to the Fermi level. Since the planes are rotated, neighbors are not on top of each other (as it is the case in the Bernal AB stacking). Interlayer interactions are then not restricted to $pp\pi$ terms but some $pp\sigma$ terms have also to be introduced. For both terms, a parameter and a characteristic length have been fitted on AA, AB, (1,3) and (1,4) cells [27] to reproduce the *ab initio* dispersion curves according to:

$$V_{pp\pi} = -\gamma_0 \exp\left(q_\pi \left(1 - \frac{d}{a}\right)\right) \quad (3)$$

$$V_{pp\sigma} = \gamma_1 \exp\left(q_\sigma \left(1 - \frac{d}{a_1}\right)\right) \quad \text{with} \quad \frac{q_\sigma}{a_1} = \frac{q_\pi}{a} \quad (4)$$

a is the nearest neighbor distance within a layer $a = 1.42$ Å and a_1 is the interlayer distance $a_1 = 3.35$ Å. With this dependence, we take first neighbors interaction in a plane equal to $\gamma_0 = 2.7$ eV and second neighbors interaction in a plane equal to $0.1 \times \gamma_0$ [28], which fixes value of the ratio q_π/a . For undoped bilayers, all p_z orbitals have the same on-site energy in both planes. We have chosen this on-site energy such that the energy of the Dirac point equals to 0 for the results detailed here.

Localization by Moiré patterns.– We have performed band structure calculations on a large number of structures. For structures that could be studied by both *ab initio* and TB methods the agreement is always excellent. For example figure 2 presents the band structure calculated with VASP and with the TB method for a small angle rotation: $(n, m) = (6, 7)$, $\theta = 5.08^\circ$ and $N = 508$. The two methods agree very well and show a decrease of the velocity by about 15 percent in that case. We

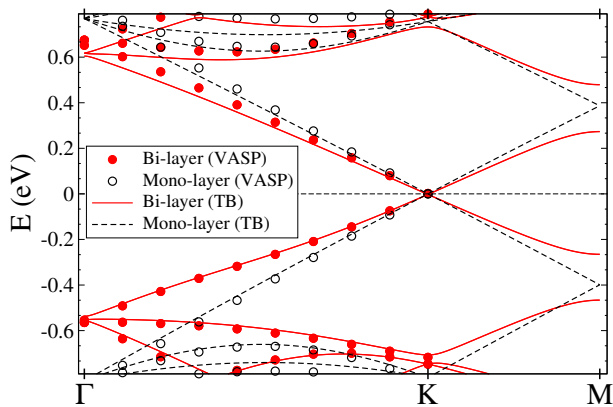


FIG. 2: (color on line) Band energy dispersion $E(\vec{k})$ in commensurate bilayer cell $(n, m) = (6, 7)$ for a rotation of $\theta = 5.08^\circ$.

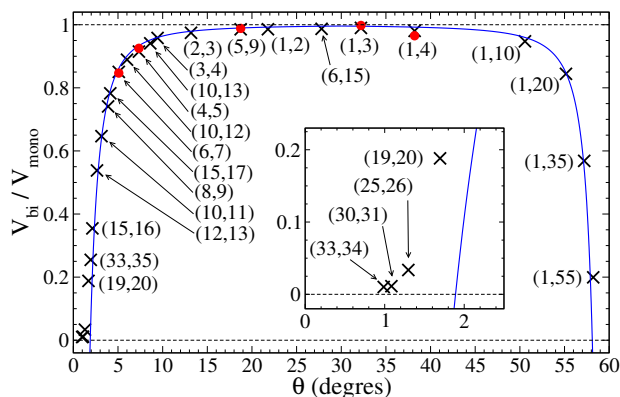


FIG. 3: (color on line) Velocity ratio $V_{\text{bi}} / V_{\text{mono}}$ for a commensurate (n, m) bilayer cell versus rotation angle θ : Circle VASP, cross TB calculations. Line is the model of Lopez dos Santos *et al.* [18]: $V_{\text{bi}} / V_{\text{mono}} = 1 - 9[\tilde{t}/(V_{\text{mono}}K \sin(\theta/2))]^2$, with $\tilde{t} = 0.11$ eV and $V_{\text{mono}}K = 2\gamma_0\pi\sqrt{3} = 9.8$ eV.

have checked that the velocity remains isotropic in the linear region up to a few percents. For angles in the range $15^\circ - 45^\circ$ and for energies, of the order of a few meV (not shown here), the dispersion is not always linear and a very small gap can even exist. Yet this small energy range is not experimentally relevant in most circumstances. We note also that for angles within a few degrees of 0° or 60° the bands become flat and the energy range in which the bands are linear decreases.

As stated above the geometry of the Moiré depends essentially on the angle θ , in the limit of small θ . This reflects in the band dispersion which depends essentially on the rotation angle θ between the two layers for all cases studied here and in particular in the small angle limit. We performed a systematic study of the renormalization of the velocity close to the Dirac point, compared to its value in a monolayer graphene, for rotation angles θ varying between 0° and 60° (figure 3).

The renormalization of the velocity varies symmetri-

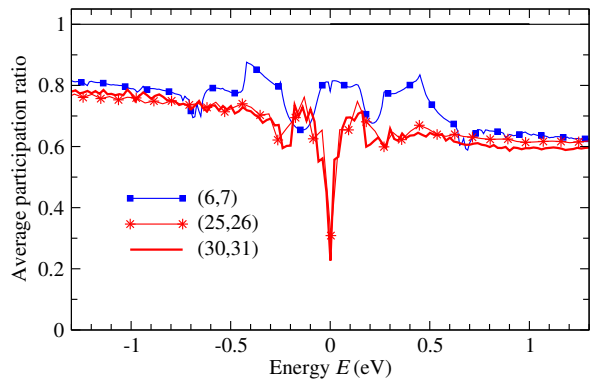


FIG. 4: (color on line) Average participation ratio $\bar{p}(E)$ at energy E for several (n, m) bilayers.

cally around $\theta = 30^\circ$. Indeed, the two limit cases $\theta = 0^\circ$ –AA stacking– and $\theta = 60^\circ$ –AB stacking– are different, but Moiré patterns when $\theta \rightarrow 0^\circ$ and when $\theta \rightarrow 60^\circ$ are similar because a simple translation by a vector transforms an AA zone to an AB zone.

Focusing on angles smaller than 30° we define three regimes as a function of the rotation angle θ . For large θ ($15^\circ \leq \theta \leq 30^\circ$) the Fermi velocity is very close to that of graphene (see figure 3). For intermediate values of θ ($3^\circ \leq \theta \leq 15^\circ$) the perturbative theory of Lopez dos Santos *et al.* [18] predicts correctly the velocity renormalization. But for the small rotation angles ($\theta \leq 3^\circ$) a new regime occurs where the velocity tends to zero. This remarkable localization regime cannot be described by the perturbative theory of Lopez dos Santos *et al.* [18].

In order to analyze this localization phenomenon we computed the participation ratio of each eigenstate $|\psi\rangle$ defined by $p(\psi) = (N \sum_i |\langle i|\psi\rangle|^4)^{-1}$. $|i\rangle$ is the p_z orbital on atom i and N is the number of atoms in a unit cell. For completely delocalized eigenstate p is equal to 1 like in graphene. On the other hand, state localized on 1 atom have a small p value: $p = 1/N$. The average participation ratio \bar{p} at energy E is presented on figure 4. For intermediate values of θ –bilayers (6,7) in figure 4– the participation ratio of states with energy close to 0 is similar to that of other states of the bilayer. For very small θ –bilayer (25,26) and (30,31) in figure 4– states with energy around 0 are strongly localized (the smallest p values down to 0.14). An analysis of spatial repartition of eigenstates, shows that these states are localized on the AA zones of the Moiré. This is illustrated on figure 5b showing 80% of the weight of an eigenstate with energy very close to 0 in the (30,31) bilayer cell. This new localization mechanism by the potential of the Moiré leads to a peak in the local density of states of atoms in the AA zone (figure 5b) whereas for Moiré due to larger angle no strong localization occurs (figure 5a). It would be interesting to check whether this localized peak can be observed in STS experiments.

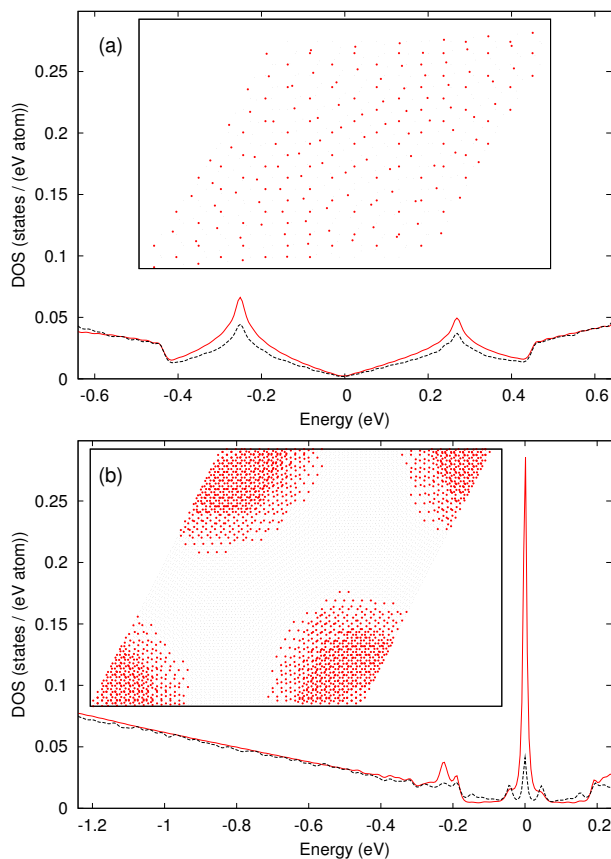


FIG. 5: (color on line) TB Local density of states on atom located at the center of a AA type zone in (a) (6, 7) and (b) (30, 31) bilayers. Inset: Repartition of a electronic state at \mathbf{K} with energy 0: Black small dots are the position of all atoms, red dots are atoms on which 80% of the electronic state is localized.

Finally we have also studied the case of asymmetric bilayers with on-site energies that are different for atoms of the two planes. Such an asymmetry can occur in graphene multilayers due to the effect of doping. In the case of Bernal AB stacking an asymmetric bilayer presents a gap but our TB calculations show that it is not the case for asymmetric rotated layers. In agreement with Lopez dos Santos *et al.* [18] we find that a difference between the on-site energies of the two layers results in a relative shift of the Dirac cones. The linear dispersion is conserved close to each Dirac point and no gap appears.

Conclusions.— In summary, by combining *ab initio* and tight-binding calculations, we have demonstrated that the dispersion relation stays linear in a rotated bilayer close to the Dirac point. Yet the velocity of electrons is renormalized. This renormalization depends essentially on a single parameter which is the rotation angle θ . For large θ , ($15^\circ \leq \theta \leq 30^\circ$), the Fermi velocity is very close to that of graphene. For intermediate values of θ ($3^\circ \leq \theta \leq 15^\circ$) the perturbative theory of Lopez dos

Santos *et al.* [18] predicts correctly the velocity renormalization. But for the small rotation angles ($\theta \leq 3^\circ$), a new regime occurs where the velocity tends to zero. This remarkable localization regime cannot be described by the perturbative theory of [18]. In this regime electrons with energy close to Dirac point are localized in AA stacked regions. We believe that this localization regime should be observable since angles as small as a fraction of a degree occur in some rotated multilayers.

Acknowledgements.— We thank C. Berger, E. Conrad, W. de Heer, P. Mallet, F. Varchon, J. Y. Veuillen, P. First for fruitful discussions. Computer time has been granted by Ciment/Phynum and S.I.R (Université de Cergy-Pontoise).

* corresponding author: guy.trambly@u-cergy.fr

- [1] K. S. Novoselov *et al.*, Science **306**, 666 (2004).
- [2] S. Y. Zhou *et al.*, Nature Phys. **2**, 595 (2006).
- [3] P. R. Wallace, Phys. Rev. **71**, 622 (1947).
- [4] K. S. Novoselov *et al.*, Nature **438**, 04233 (2005).
- [5] Y. Zhang, Y.-W. Tan, H. L. Stormer and P. Kim, Nature **438**, 04235 (2005).
- [6] K. S. Novoselov *et al.*, Science **315**, 1379 (2007).
- [7] A. K. Geim, K. S. Novoselov, Nature Materials **6**, 183 (2007). A. K. Geim, K. S. Novoselov, Nature Materials **6**, 183 (2007).
- [8] A. de Martino, L. Dell'Anna, R. Egger, Phys. Rev. Lett. **98**, 066802 (2007).
- [9] T. Ando, T. Nakanishi, J. Phys. Soc. Jpn, **67**, 1704 (1998).
- [10] C. Berger *et al.*, Science **312**, 1191 (2006).
- [11] W. A. de Heer *et al.*, Solid State Com. **143**, 92-100 (2007).
- [12] C. Berger *et al.*, J. Phys. Chem. B **108**, 19512 (2004).
- [13] X. Wu *et al.*, Phys. Rev. Lett. **98**, 136801 (2007).
- [14] I. Brihuega *et al.*, Phys. Rev. Lett. **101**, 206802 (2008).
- [15] C. H. Park *et al.*, Nature **4**, 213 (2008).
- [16] M. Barbier *et al.*, Phys. Rev. B **79**, 155402 (2009).
- [17] J. Hass *et al.*, Phys. Rev. Lett. **100**, 125504 (2008).
- [18] J. M. B. Lopez dos Santos, N. M. R. Peres, A. H. Castro Neto, Phys. Rev. Lett. **99**, 256802 (2007).
- [19] S. Shallcross, S. Sharma, O. A. Pankratov, Phys. Rev. Lett. **101**, 056803 (2008).
- [20] S. Latil, V. Meunier, L. Henrard, Phys. Rev. B **76**, 201402(R) (2007).
- [21] F. Varchon, P. Mallet, J.-Y. Veuillen, L. Magaud, Phys. Rev. B **77**, 235412 (2008).
- [22] Z. Y. Rong, P. Kuiper, Phys. Rev. B **48**, 17427 (1993).
- [23] J. M. Campanera, G. Savini, I. Suarez-Martinez, M. I. Heggie Phys. Rev. B **75**, 235449 (2007).
- [24] G. Kresse and J. Hafner, Phys. Rev. B **47**, 558 (1993)
- [25] J. P. Perdew and Y. Wang, Phys. Rev. B **33**, 8800 (1986)
- [26] G. Kresse and J. Hafner, J. Phys. Condens. Matter **6**, 8245 (1994)
- [27] G. Trambly de Laissardière, D. Mayou, L. Magaud, unpublished.
- [28] A. H. Castro Neto *et al.*, Rev. Mod. Phys. **81**, 109 (2009).